Assessment of Propeller Modeling Approaches for Aerodynamic Simulations

Dennis Keller⋆ †, *Sebastian Spinner*⋆, *Arne Stuermer*⋆ *and Jack Park*§
⋆*DLR German Aerospace Center*
Lilienthalplatz 7, 38108 Braunschweig
dennis.keller@dlr.de
§*DLR German Aerospace Center*
Nöthnitzer Str. 46b, 01187 Dresden
†Corresponding author

Abstract

Accurate modeling of propeller performance is crucial for the reliable aero-propulsive analysis of emerging aircraft configurations, particularly those employing distributed propulsion for improved efficiency and reduced emissions. This study evaluates the performance of propeller models – actuator disk and virtual blade – embedded within the DLR's TAU and CODA CFD codes, comparing results to URANS simulations and wind tunnel experiments using the TU Delft ProWim propeller test case. The accuracy of both global performance parameters and propeller slipstream characteristics was assessed. Results indicate that while lower-fidelity models generally predict higher thrust and power coefficients, they demonstrate acceptable agreement with URANS and experimental data at low advance ratios. Discrepancies increase significantly at higher advance ratios, and both models exhibit inaccuracies in representing the propeller slipstream, particularly regarding blade tip loading and flow separation. The investigation confirms that incorporating modeling details, such as tangential induced velocities, significantly improves accuracy, especially at low advance ratios. These findings highlight the importance of careful model selection and parameter tuning for reliable aero-propulsive simulations of future propeller-driven aircraft.

1. Introduction

With the push towards more sustainable aviation, there is even more focus on energy efficiency in aircraft design. One of the most promising options for short to medium range aircraft is the utilization of propellers for thrust generation, which offer superior efficiency compared to turbofan engines at low and moderate cruise speeds. The propeller's advantages in terms of fuel consumption and emissions reduction make it an attractive option for airlines and aircraft manufacturers seeking to minimize their environmental footprint. To further reduce climate impact electrification of the power train is seen as a promising approach. The better scalability of electric motors compared to gas turbine engines and the potentially less complex power distribution via electric cables allow for new propulsor integration concepts such as distributed propulsion. These new concepts typically feature a closer coupling of the propulsors with the airframe. As a result, not only the precise evaluation of the propeller efficiency but also of the propeller slipstream is crucial in order to predict the aero-propulsive performance of such designs reliably. The correct representation of the propeller slipstream is also important for the investigation of high-lift cases, where deviations can affect the maximum angle of attack, the maximum lift coefficient, and even the stall behavior. Accurate and efficient propeller modeling approaches within computational fluid dynamics (CFD) simulations are therefore of great value.

Building on previous validation efforts[1],[2], this study evaluates the performance of propeller models embedded in *DLR*'s TAU codes and the evolving CODA (CFD Software by *ONERA*, *DLR* and *Airbus*) code, with a focus on their application to integrated wing-nacelle-propeller configurations. Specifically, the accuracy of global performance parameters of the propeller is assessed. Additionally wake data that is relevant for the aerodynamic performance of wings, which are potentially located downstream of the propeller is analysed. The aim of the study is to provide insights into the most effective modeling approaches for aero-propulsive assessments of propeller-driven aircraft configurations and quantify the impact of model deficiencies.

Windtunnel Run	v [m/s]	n [1/s]	J [-]
1-1	39.2	260.8	0.6338
2-2	39.2	226.0	0.7317
1-23	39.2	178.4	0.9267
1-18	39.2	161.4	1.0245

Table 1: Studied test cases

2. Methods

To test the different propeller modeling approaches in numerical simulations, a wind tunnel experiment published by *Sinnige et.al*[3] was selected as reference. The tested propeller has a diameter of 0.237 m with four blades at a blade pitch angle of 23.9° at 75 % of the radius. The onset flow velocity is 39.2 m/s at wind tunnel conditions. Four test cases were selected from the wind tunnel test matrix, allowing to assess propeller metrics over a wide range of the performance envelope of the propeller. Spanning from low to high advance ratios the test cases are summarized in Table 1. The specific advance ratios were thereby achieved by alteration of the propeller's rotational speed. The wind tunnel run number corresponds to the polar and run number in the wind tunnel data.

2.1 Geometry

The geometry used in the CFD computations closely resembles the model used in the wind tunnel experiment[3] including the spinner, nacelle and sting. The wind tunnel wall is replaced by a symmetry plane. Depending on the numerical approach, the propeller's geometry is either fully resolved including the exact blade geometry (URANS), represented by a zero thickness disk at 0.5 chord lengths on the spinner (actuator disk), or modeled via a disk of cells with an axial extent of one cell located at the same axial location as the actuator disk (virtual blade model). Figure 1 illustrates the geometry for the actuator disk (red plane) computations.

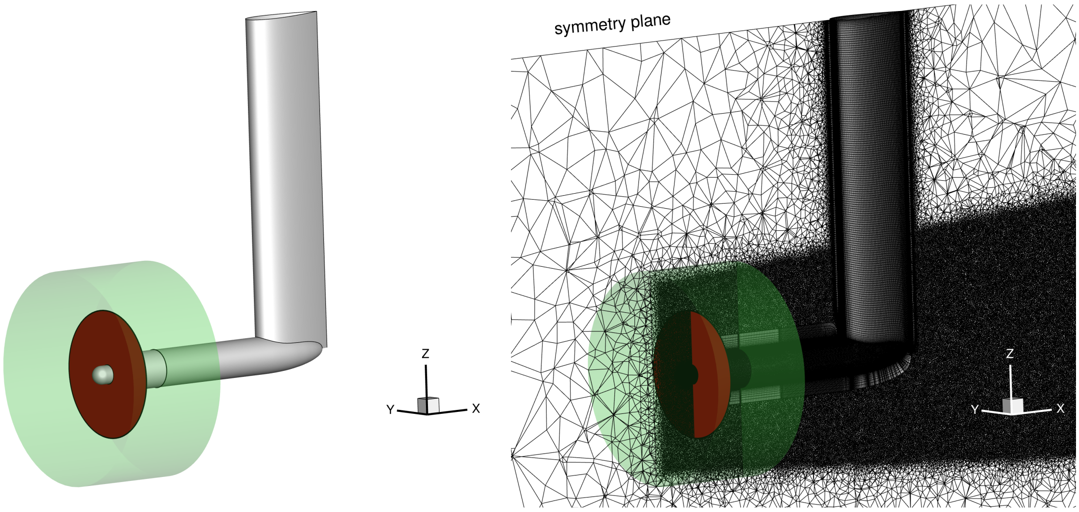

(a) Geometry for the CFD analyses

(b) Surface and volume mesh for an iso-Y cutting plane along the propeller axis of the actuator disk mesh

Figure 1: Geometric setup and meshing overview for the ProWim propeller test case

2.2 Meshing

The meshes were created with a semi-automated hybrid meshing approach using the Centaur mesh generator[4]. Centaur first creates a surface grid based on triangles and quads. From the surface grid, a near-field volume mesh is generated with an advancing-layer algorithm. Due to the characteristics of the surface mesh, the near-field mesh consists of prism and hexahedra stacks. Outside of the near-field mesh, the computational domain is filled with tetrahedra. To minimise the influence of the grid on the results of the different propeller modeling methods as much as possible, a modular mesh approach was chosen. The majority of the volume mesh is thereby kept identical for all propeller modeling methods. Only the mesh in the propeller region itself, which has to be modified according to the individual propeller modeling method, is remeshed. The green box in Fig. 1 illustrates the boundaries of the propeller module that is being replaced. Figure 1(b) depicts the resulting surface and volume mesh in a cutting plane along the propeller axis (Y=const.) for the actuator disk approach.

2.3 Propeller Modeling

In this study, three distinct approaches to modeling a propeller in numerical simulations were evaluated and compared. The first approach, known as the actuator disk (AD) method, is based on blade element momentum theory and incorporates a vortex model to account for induced velocities in the circumferential direction. However, the model does not include a tip-loss correction. The resulting forces are imposed on a disk of zero thickness, leading to a discontinuity in both the pressure and flow direction, but a continuous evolution of velocity.[1],[5]

An alternative approach is the virtual blade model (VBM), which simplifies the propeller representation similar to the AD model. The VBM, originally formulated by *Zori and Rajagopalan*[6], relies on a dataset of sectional lift and drag coefficients obtained from 2D RANS simulations of the blade sections. By combining this dataset with blade element theory, volume-specific source terms can be computed and imposed on the flow field in the region swept by the propeller blades. Note that, in contrast to the AD mode, the VBM does not incorporate any vortex model. A tip-loss correction is not included either.

The highest-fidelity methodology is achieved by fully resolving the flow around the rotating blade surfaces of the propeller. This is accomplished by utilizing mesh rotation and Chimera capabilities, which enable the rotation of the propeller geometry against a stationary background mesh[7],[8]. This approach provides the most detailed and accurate representation of the propeller flow, but is also the most computationally intensive.

2.4 Flow Solver

To investigate the propeller modeling capabilities, two different flow solvers were employed: the DLR TAU Code and the CFD Software by ONERA, DLR, and Airbus (CODA). The DLR TAU Code is a well-established, unstructured cell-vertex based finite volume solver, widely used in aerospace applications[9]. It has a proven track record of successfully simulating complex flows, including those involving propellers[10],[11] and contra-rotating open rotors[12],[13],[14].

CODA is the computational fluid dynamics (CFD) software being developed as part of a collaboration between the French Aerospace Lab ONERA, the German Aerospace Center (DLR), Airbus, and their European research partners. CODA is jointly owned by ONERA, DLR and Airbus. The solver operates on unstructured meshes applying a cell-centered metric and combines established finite-volume (FV) schemes with high-order Discontinuous-Galerkin (DG) methods. It was designed for efficient simulations on highly parallel and heterogeneous HPC architectures, applying modern software techniques.[15]

Although both solvers were used to test the propeller modeling methods, not all methods were available for both solvers at the time of writing. The actuator disk and unsteady RANS modeling were applied using the DLR TAU Code, while the virtual blade model source term approach was used in conjunction with CODA. This study provides a comprehensive comparison of different propeller modeling methods, including sensitivity analyses, with results obtained using both the DLR TAU Code and CODA, offering a first glimpse into the potential of CODA for propeller simulations.

3. Results

3.1 Best Practice

In the following section, the results of the actuator disk and virtual blade model approaches are compared to the results of the URANS computations and the wind tunnel experiment. The results were obtained by utilizing the current "best practice" for the individual models. Accordingly, the sectional aerodynamic input data were created with an extended 2D method[1] that considers the inertial effects of the rotational motion. Since the effect depends on the rotational speed, an individual set of input data was created for each case.

3.1.1 Global performance

The plots in Fig. 2 show the propeller performance for the different approaches at a constant pitch. The propeller pitch for each method was set to match the pitch from the wind tunnel experiment. Considering the power coefficient in Fig. 2(a) and the thrust coefficient in Fig. 2(b) one can see that all models accurately reflect the trend of the wind tunnel data. All models show a decrease in power and thrust with increasing advance ratio with a very similar gradient. The URANS approach thereby also accurately matches the absolute values of the wind tunnel experiment. In contrast, the AD and VBM models show significantly higher values for power and thrust compared to the wind tunnel data, with the VBM model showing the highest absolute deviations from the wind tunnel experiment.

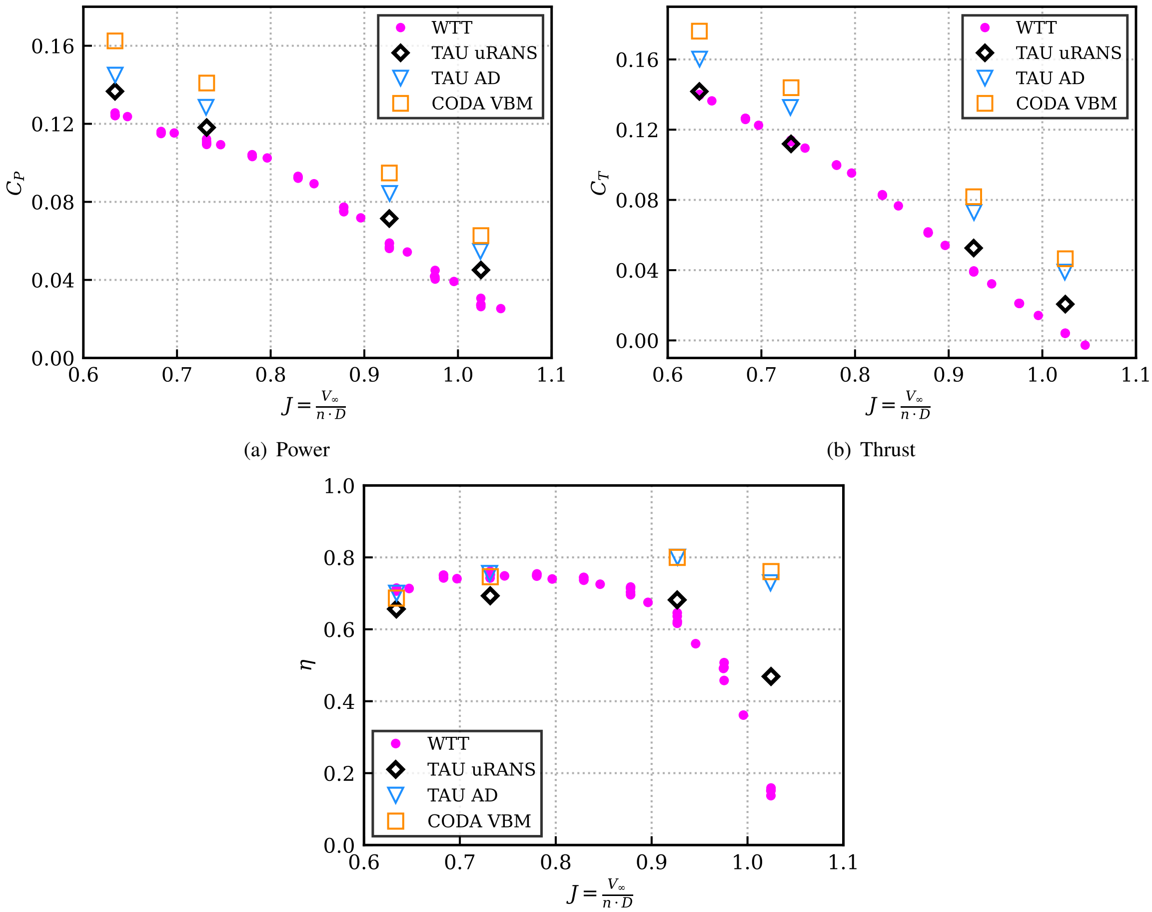

(a) Power (b) Thrust

(c) Efficiency

Figure 2: Propeller performance comparison of wind tunnel data and numerical simulation methods

Looking at the resulting efficiency curve in Fig. 2(c), it is noticeable that all models still agree well with the experimental data at moderate advance ratios. However, if the advance ratio is increased, the deviations between the data of the numerical simulations and the data of the wind tunnel experiment also increase. Only the URANS approach is able to reproduce the course of the wind tunnel data at higher degrees of progress, whereby the deviations are already significant at the highest advance ratio investigated. Both the AD and the VBM model show a massive overestimation of the efficiency at advance ratios above 0.9.

3.1.2 Radial distributions

Thrust Distribution Figure 3 compares the radial $C'_{T,blade}$ distribution of the actuator disk computations with those of the URANS simulations. For the unsteady simulations, a solid black line is plotted for each test case, which represents the mean thrust distribution of the blade as averaged for one full propeller revolution. Also included are light gray lines, which show the deviations from this mean value for selected instantaneous snapshots or azimuthal positions during the blades rotation. Thrust distributions from the VBM approach were not available. Generally, the plots demonstrate a good agreement between the AD and URANS methods for all cases between $0.4 \leq r/R \leq 0.75$. At lower r/R values, notable differences can be observed. Here, the mean C'_T values of the URANS become negative indicating flow separation. This correlates well with the wind tunnel experiment, where total pressure losses related to flow separation on the inboard part of the blade identified[16]. As shown in the example of an instantaneous snapshot of the blade suction side flow topology from the URANS simulations of run 1-1 (Fig. 4), this detached flow impacts the trailing edge region of the blade from the hub up until around 40 %. It is evidently primarily triggered by the cylindrical root section at the hub itself and further amplified by the interaction of the propeller slipstream with the relatively blunt forward portion of the nacelle/sting in the inboard region of the propeller. The flow separation is highly unsteady as the wide range of local $C'_{T,blade}$ values of the transient data reveal. The AD method also predicts negative $C'_{T,blade}$ values attributed to flow separation.

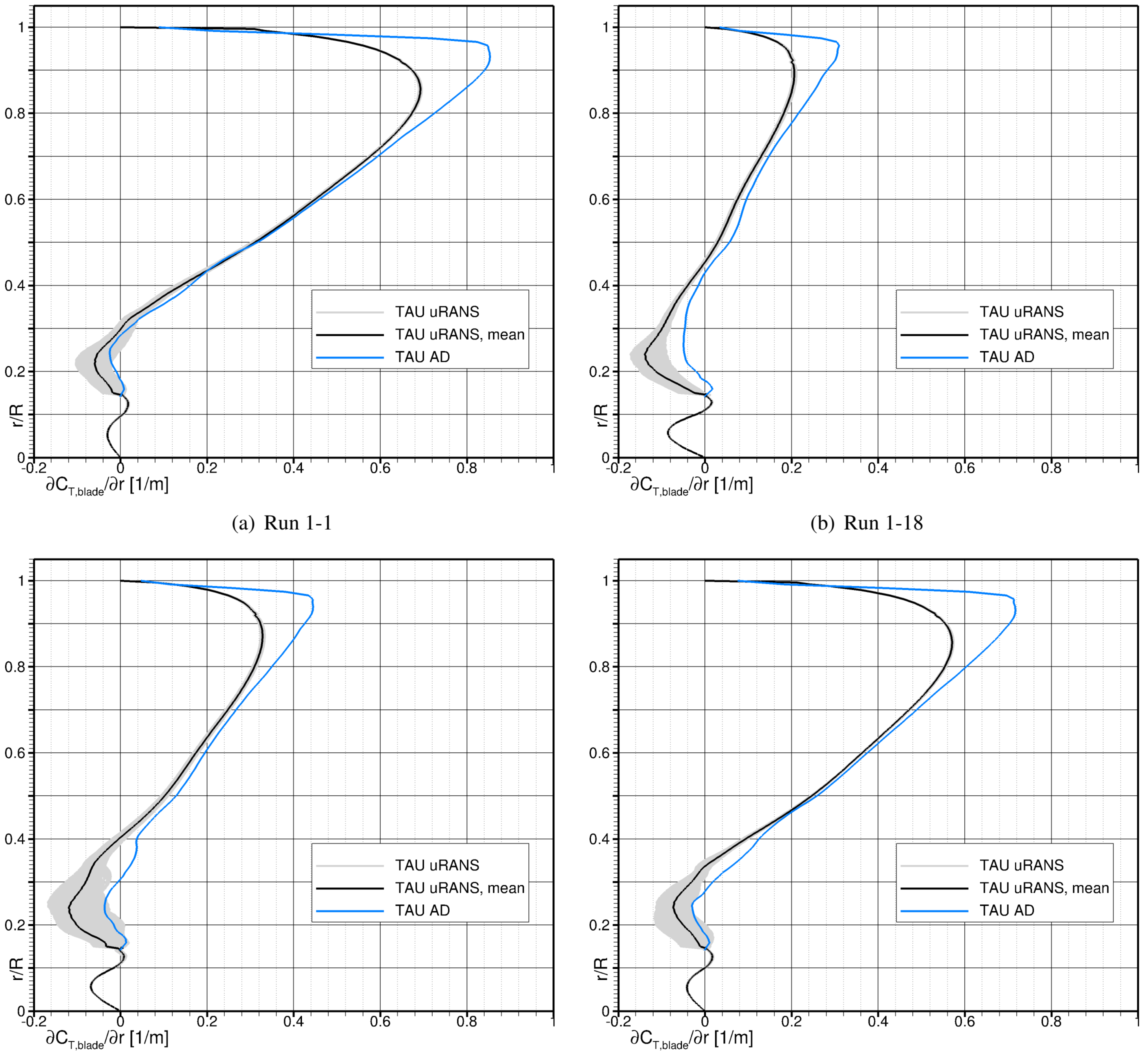

(a) Run 1-1 (b) Run 1-18

(c) Run 1-23 (d) Run 2-2

Figure 3: Comparison of the radial blade C_T distributions for the TAU-based simulations

However, the adverse effect on the thrust distribution is significantly weaker compared to the URANS in particular for run 1-18 and 1-23, which yield the lowest propeller thrust of all the investigated cases. Besides the discrepancies at the blade root, significant differences can be observed for the blade tip region. Here, the AD method generally overpredicts the local $C'_{T,blade}$ as the 3D effect - i.e. the induced angle of attack - of the finite blade is not considered correctly.

Wake Data In the following paragraph, flow field data by means of total pressure coefficient $C_{p,t}$ and swirl angle (only numerical results) extracted at $\Delta X = 0.15\,R$ downstream of the propeller and a circumferential position of $\phi = 180°$ are compared. As for the thrust distributions discussed in the previous paragraph, the data shown from the URANS simulations represents the mean values for the pressure coefficient and swirl angles as obtained through an averaging of the flowfield data for one complete propeller revolution.

Figure 5 depicts radial total pressure coefficient distributions for the investigated cases. It shall be noted that for some cases wind tunnel data was not available for the exact advance ratio. In this case, available experimental data of the advance ratio that matches best with the advance ratio of the run is plotted. Keeping this in mind, the $C_{p,t}$ distributions of the URANS and the experiment match well. With regard to the propeller models, again, the agreement

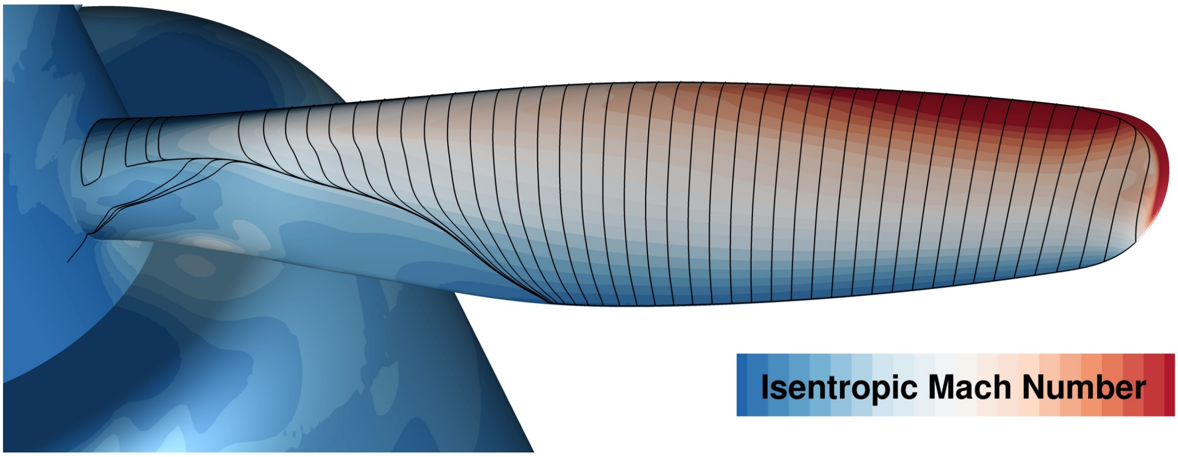

Figure 4: Example of the ProWim propeller test case flow topology in the URANS simulations, showing the flow separation occurring at the blade hub for run 1-1

between the AD method and the URANS data is good for $0.45 \leq r/R \leq 0.75$. At lower and higher r/R, larger differences can be observed that correlate to the differences seen for the thrust distributions. The $C_{p,t}$ distributions of the VBM method generally follow this trend. However, notable anomalies can be seen in particular for the runs with the highest propeller thrust (run 1-1 & 2-2). This waviness is most pronounced around $r/R \approx 0.5$.

Figure 6 compares the swirl distribution of the numerical simulations. Again, the results of the TAU AD method and the CODA VBM implementation generally agree well with the URANS data with slightly higher differences being found for the latter. Similar to the $C_{p,t}$ distributions, the swirl distributions indicate higher discrepancies at the blade root and tip. Moreover, the anomalies in terms of local overshoots can again be observed in the VBM distributions.

3.2 Sensitivities

In order to assess the effect of individual propeller modeling aspects, additional computations were performed with the actuator disk approach. Deviating from the "best practice" approach (Sec. 3.1), the following changes were made in the computations:

- **2D:** The sectional input dataset that feeds the actuator disk was created with conventional 2D computations neglecting inertial effect.
- **BEM:** The self-induced tangential velocities of the blades that are considered in the BEMT method in order to compute the local effective angle of attack of the blade were set to zero, effectively transforming the BEMT method into a BEM method.
- **Target thrust:** Instead of using the design blade pitch, the blade was rotated to achieve the thrust value measured in the wind tunnel experiment. This approach shall resemble the typical actuator disk usage for simulating integrated wing-nacelle-propeller configurations, where typically a given target thrust or propulsive power is set.

3.2.1 Global performance

Figure 7 presents global propeller performance metrics for computations using the AD approach, as described previously. For reference, the "best practice" TAU AD and the TAU URANS data from Fig. 2 are plotted identically in this figure. Examining the power coefficient in Fig. 7(a), the "best practice" AD model closely aligns with the URANS simulation. Neglecting inertial effects (2D) or tangential velocities (BEM) yields slightly higher power coefficients. Fig 7(b) displays the thrust coefficient for each model. Consistent with observations in Fig. 2(b), the AD model generally overpredicts thrust, a trend not significantly affected by the 2D or BEM variants. As expected, running the AD model in *target thrust* mode results in a thrust value that precisely matches the wind tunnel data, with a corresponding reduction in power coefficient compared to the other TAU AD variants.

The impact of varying AD modeling on the propeller efficiency is summarized in Fig. 7(c). Consistent with previous results, the 2D and BEM variants have minimal influence on efficiency. However, trimming the blade to reach a specific thrust (target thrust) improves the reproduction of the overall efficiency trend with varying advance ratio.

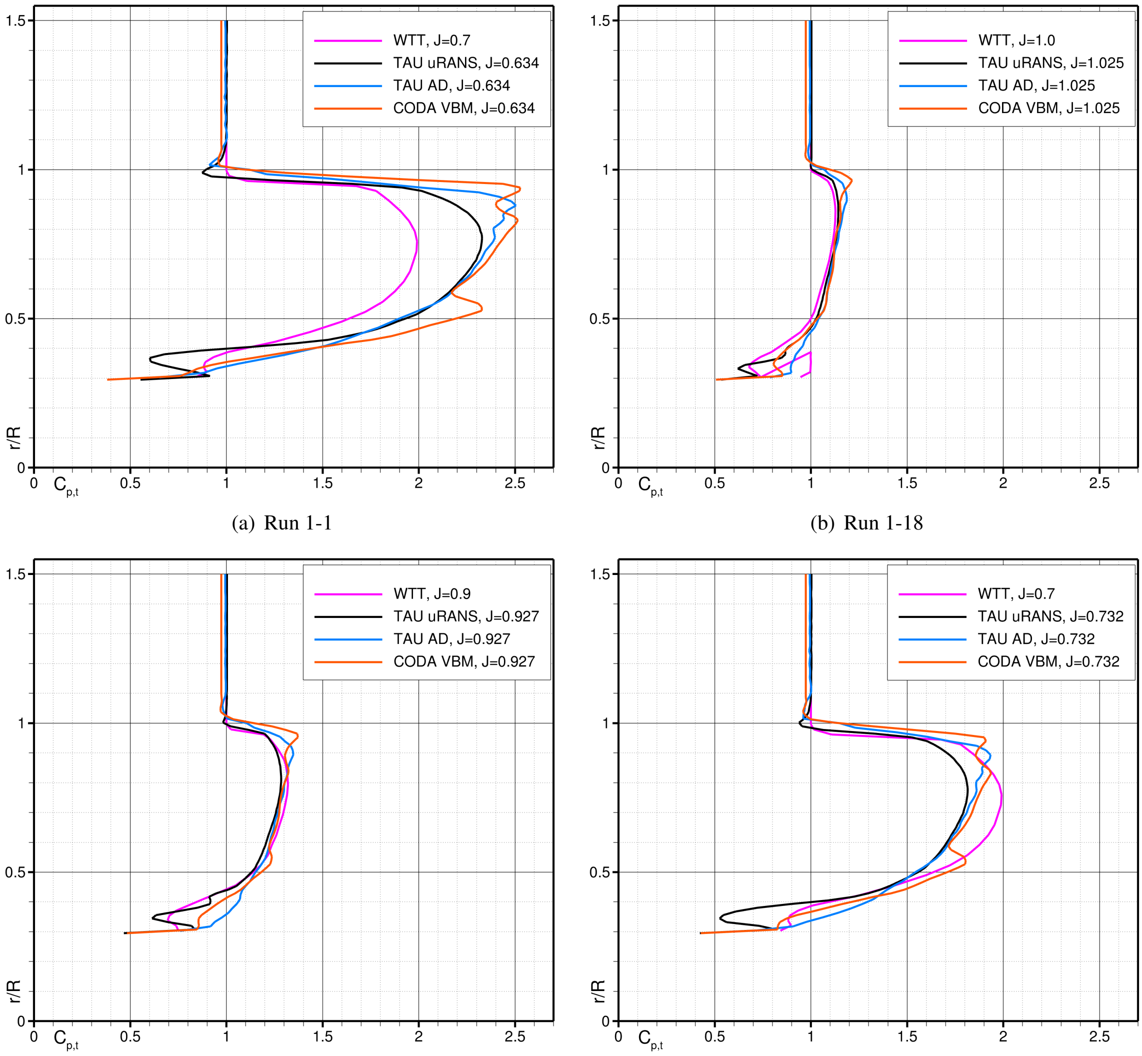

(a) Run 1-1 (b) Run 1-18

(c) Run 1-23 (d) Run 2-2

Figure 5: Comparison of CFD results for the radial $C_{p,t}$ distribution in the slipstream at $0.15R$ downstream of propeller

3.2.2 Radial distributions

Thrust Distribution Figure 8 illustrates the influence of the modeling aspects on the radial $C'_{T,blade}$ distribution of each blade. Comparing the "best practice" approach (blue line) with the "2D" (green line) and "BEM" (red line) approach confirms the beneficial impact of incorporating these improved physical modeling details in an actuator disk simulation, with the magnitude of the effect differing from case to case. The basic trends of the distributions including the overestimation of the local thrust at the blade tip and the underestimation of the effect linked to the flow separation at the blade root remain however unchanged. The largest differences can be observed for the "target thrust" computations. Due to the previously discussed deficiency in accurately predicting the local thrust at the blade root and tip, the blade pitch angle is decreased by up to $\Delta\beta_{075} = -1.7°$ (run 1-23) in order to match the thrust measured in the experiment. The differences may be particularly large for this specific test case due to the notable flow separation that are thought to be a peculiarity not existent in typical applications.

Wake Data As expected, the influence of the modeling aspects on the radial total pressure (coefficient) distribution downstream of the propeller correlates well with the influence on the thrust distributions as Fig. 9 demonstrates. Without either considering the inertial effects or the induced tangential velocities, the $C_{p,t}$ curves are shifted to higher values for all cases. Most notably thereby is the effect of the induced tangential velocities at high thrust levels (run 1-1 & run 2-2). Here, $C_{p,t}$ within the wake is increased by up to 5 % (run 1-1). In contrast targeting the thrust from the experiment lowers the wake $C_{p,t}$ substantially by up to 8 % (run 1-1 & run 1-23). Compared to both of these impacts,

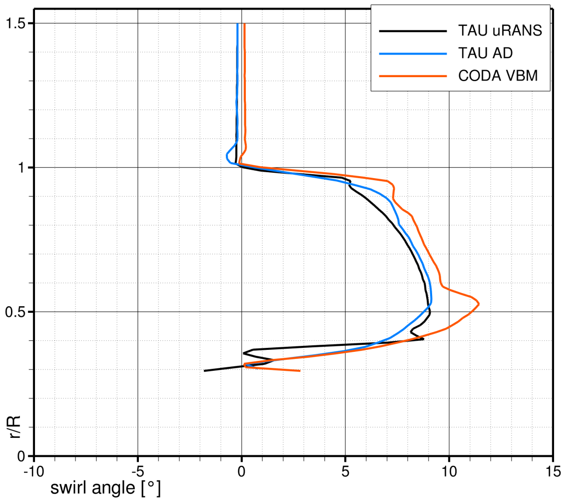

(a) Run 1-1

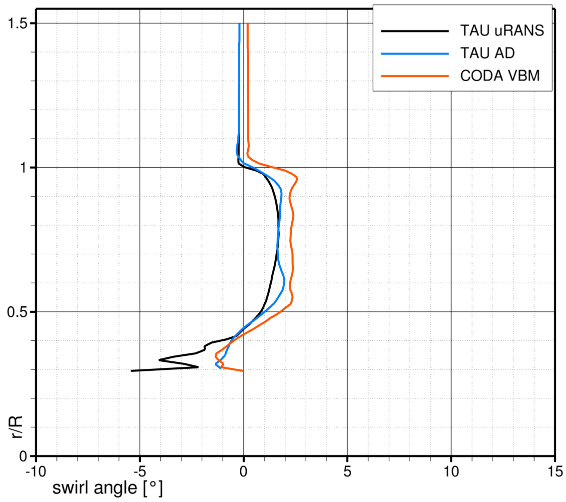

(b) Run 1-18

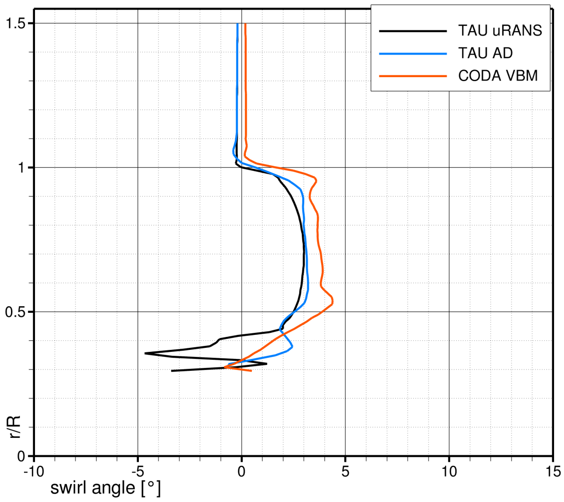

(c) Run 1-23

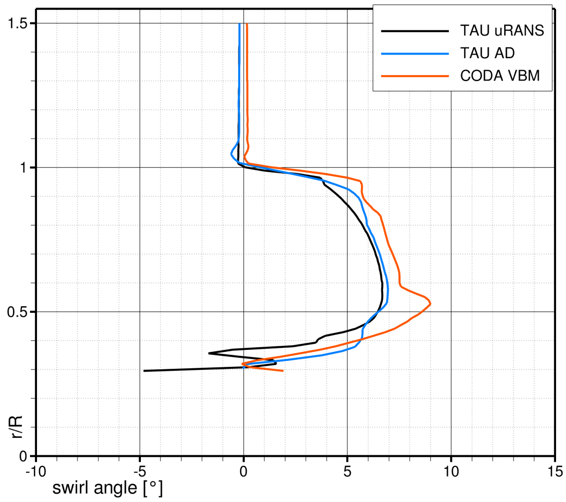

(d) Run 2-2

Figure 6: Comparison of CFD results for the radial swirl distribution in the slipstream at $0.15R$ downstream of propeller

the effect of considering inertia effects in the input data appears to be rather negligible.

Fig. 10 shows the effect of the modeling details on the swirl angle within the slipstream. Neglecting the induced tangential velocities as well as utilizing conventional 2D RANS simulation for the creation of the actuator disk input data both generally lead to an overestimation of the swirl angle. The impact of the induced tangential velocities is thereby stronger compared to the type of input data. Neglecting both causes a deviance of up to 1 degree. The computations at target thrust yield a generally lower swirl angle except for the propeller tip and the hub region, which is affected by flow separation.

4. Conclusion

This study compares CFD-based propeller performance predictions for TU Delft's ProWim propeller test case as obtained using the DLR TAU code with an actuator disk and CODA with a virtual blade model, to URANS simulation results obtained with TAU as well as the TU Delft wind tunnel test experimental data. The URANS simulation data exhibits good agreement with the wind tunnel data, with the largest discrepancies in propeller efficiency occurring at high advance ratios. Generally, the actuator disk and virtual blade models predict higher thrust and power coefficients. However, both demonstrate good agreement with URANS in terms of efficiency at low advance ratios, with differences increasing considerably as the advance ratio rises.

Regarding the propeller slipstream, the lower-fidelity models generally agree well with the URANS simulations, although the virtual blade model exhibits larger deviations in swirl angle. Furthermore, the virtual blade model introduces anomalies in total pressure and swirl in the mid-span region of the propeller blades at low advance ratios. Both models share a tendency to significantly overpredict the local load at the blade tip, leading to exaggerated total pressure and swirl in the slipstream. Conversely, they underpredict the effect of local flow separation at the blade root, as observed in the slipstream's total pressure and swirl distributions.

The study also confirms that incorporating modeling details – such as induced velocities via momentum theory and inertia effects of the rotation in the sectional input data – improves accuracy. While the impact of inertia effects is minor, accounting for tangential induced velocities is more significant, particularly at low advance ratios.

To further increase the accuracy of the lower-fidelity propeller models - in particular the local load and slipstream conditions at the blade tip - the implementation of a tip-loss correction is highly recommended.

References

[1] A. Raichle. "Flux Conservative Discretization of the Actuator Disk Model as a Discontinuity Surface". PhD thesis. Technical University Braunschweig, 2017.

[2] M. Schollenberger and T. Lutz. "Comparison of Different Methods for the Extraction of Airfoil Characteristics of Propeller Blades as Input for Propeller Models in CFD". In: *New Results in Numerical and Experimental Fluid Mechanics XIII*. Ed. by Andreas Dillmann et al. Cham: Springer International Publishing, 2021, pp. 24–34.

[3] T. Sinnige et al. "Unsteady Pylon Loading Caused by Propeller-Slipstream Impingement for Tip-Mounted Propellers". In: *Journal of Aircraft* 55.4 (2018), pp. 1605–1617.

[4] CentaurSoft. "Centaur Hybrid Grid Generation System". In: [online web site], URL: http://www.centaursoft.com. [retrieved 20 March 2025].

[5] A. Raichle, S. Melber-Wilkending, and J. Himisch. "A New Actuator Disk Model for the TAU Code and Application to a Sailplaine with a Folding Engine". In: *New Results in Numerical and Experimental Fluid Mechanics VI*. Ed. by Cameron Tropea et al. Berlin, Heidelberg: Springer Berlin Heidelberg, 2008, pp. 52–61. ISBN: 978-3-540-74460-3.

[6] L. A. J. Zori and R. G. Rajagopalan. "Navier-Stokes Calculations of RotorAirframe Interaction in Forward Flight". In: *Journal of the American Helicopter Society* 40.2 (1995), pp. 57–67. ISSN: 2161-6027. DOI: doi: 10.4050/JAHS.40.57.

[7] A. Stuermer. "Validation of an Unstructured Chimera Grid Approach for the Simulation of Propeller Flows". In: *22nd Applied Aerodynamics Conference and Exhibit*. AIAA 2004-5289. Providence, RI, USA, Aug. 2004. DOI: 10.2514/6.2004-5289. URL: https://arc.aiaa.org/doi/abs/10.2514/6.2004-5289.

[8] A. Stürmer. "CFD Validation of Unsteady Installed Propeller Flows Using the DLR TAU-Code". In: *1st CEAS European Air and Space Conference*. Ed. by DGLR. Vol. 3. Jahrbuch. DGLR, Sept. 2007. URL: https://elib.dlr.de/52122/.

[9] T. Gerhold. "Overview of the Hybrid RANS Code TAU". In: *MEGAFLOW – Numerical Flow Simulation for Aircraft Design*. Ed. by N. Kroll and J.K. Fassbender. Springer Berlin Heidelberg, 2005, pp. 81–92.

[10] C. Lenfers, N. Beck, and M. Bauer. "Propeller and Active High Lift Wing Interaction in Experiment and Simulation". In: *New Results in Numerical and Experimental Fluid Mechanics X* 132 (2016), pp. 51–61.

[11] E. W. M. Roosenboom, A. Stuermer, and A. Schroeder. "Advanced Experimental and Numerical Validation and Analysis of Propeller Slipstream Flows". In: *Journal of Aircraft* 47.1 (2010), pp. 284–291. DOI: 10.2514/1.45961. URL: https://doi.org/10.2514/1.45961.

[12] C. O. Marquez Gutierrez et al. "Validation of Actuator Disk Simulations of CROR Propulsion Systems at Low-Speed Flight Conditions". In: 2012-2787. American Institute of Aeronautics and Astronautics. New Orleans, USA, 2012.

[13] A. Stuermer. "Validation of Installation Effect Predictions Through Simulations of CRORs at Low-Speed Flight Conditions". In: *AIAA Aviation 2015*. AIAA 2015-2886. Dallas, TX, USA, 2015.

[14] A. Stuermer and R. A. D. Akkermans. "Validation of Aerodynamic and Aeroacoustic Simulations of Contra-Rotating Open Rotors at Low-Speed Flight Conditions". In: *AIAA Aviation 2014*. AIAA 2014-3133. Atlanta, GA, USA, 2014.

[15] P. S. Volpiani et al. "Aircraft Simulations Using the New CFD Software from ONERA, DLR and Airbus". In: *Journal of Aircraft* 61.3 (2024), pp. 857–869.

[16] T. Sinnige et al. “Wingtip-Mounted Propellers: Aerodynamic Analysis of Interaction Effects and Comparison with Conventional Layout”. In: *Journal of Aircraft* 56.1 (2019), pp. 295–312. DOI: 10.2514/1.C034978.

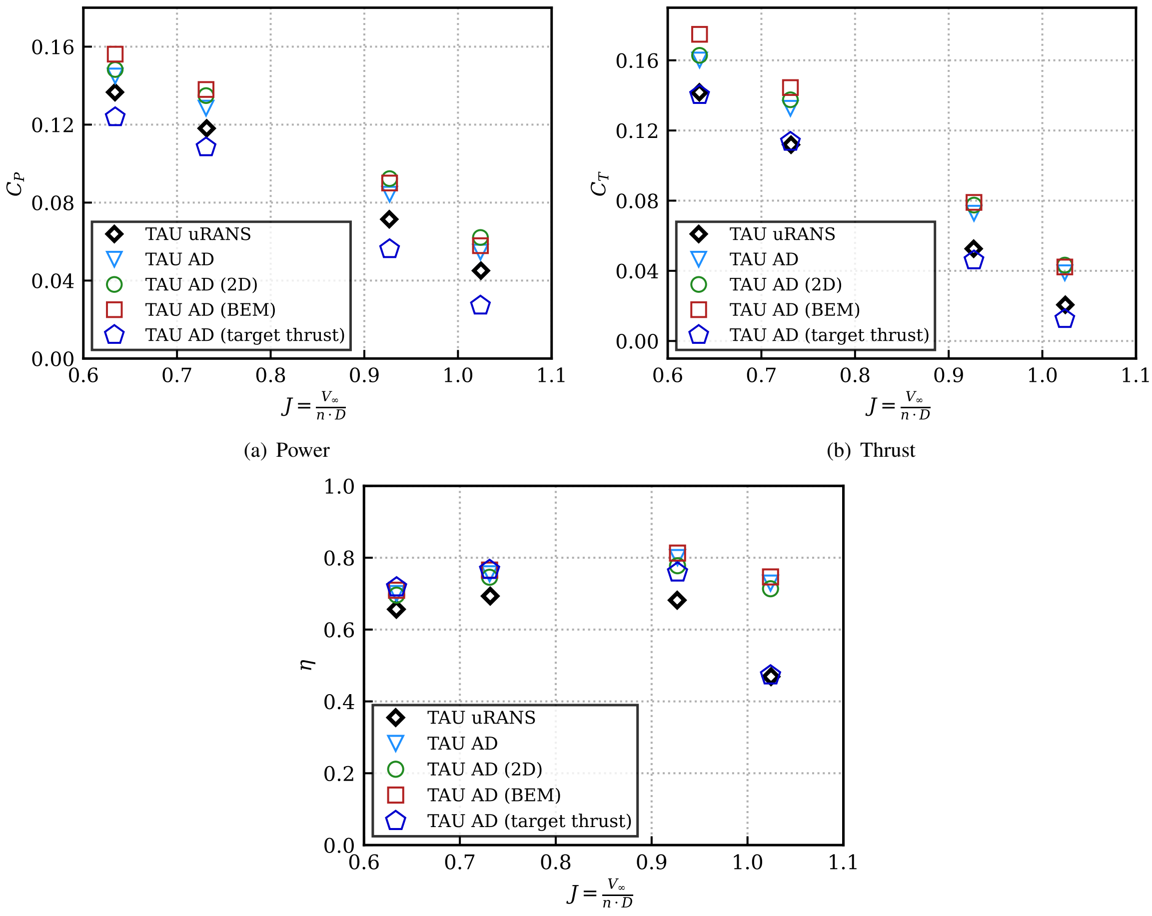

(c) Efficiency

Figure 7: Comparison of propeller performance predictions using different AD modeling approaches

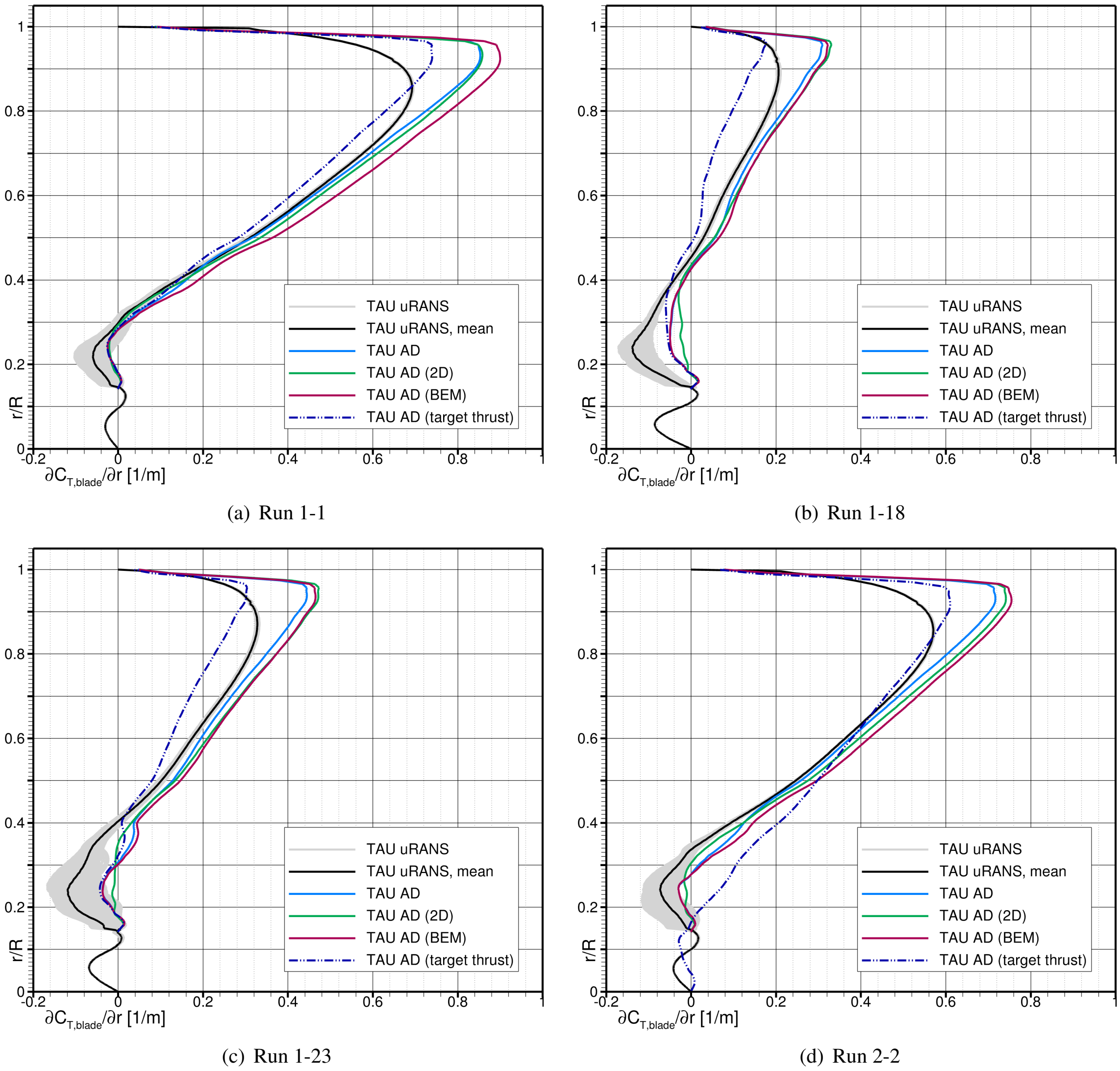

Figure 8: Comparison of the radial blade C_T distributions for different AD modeling approaches

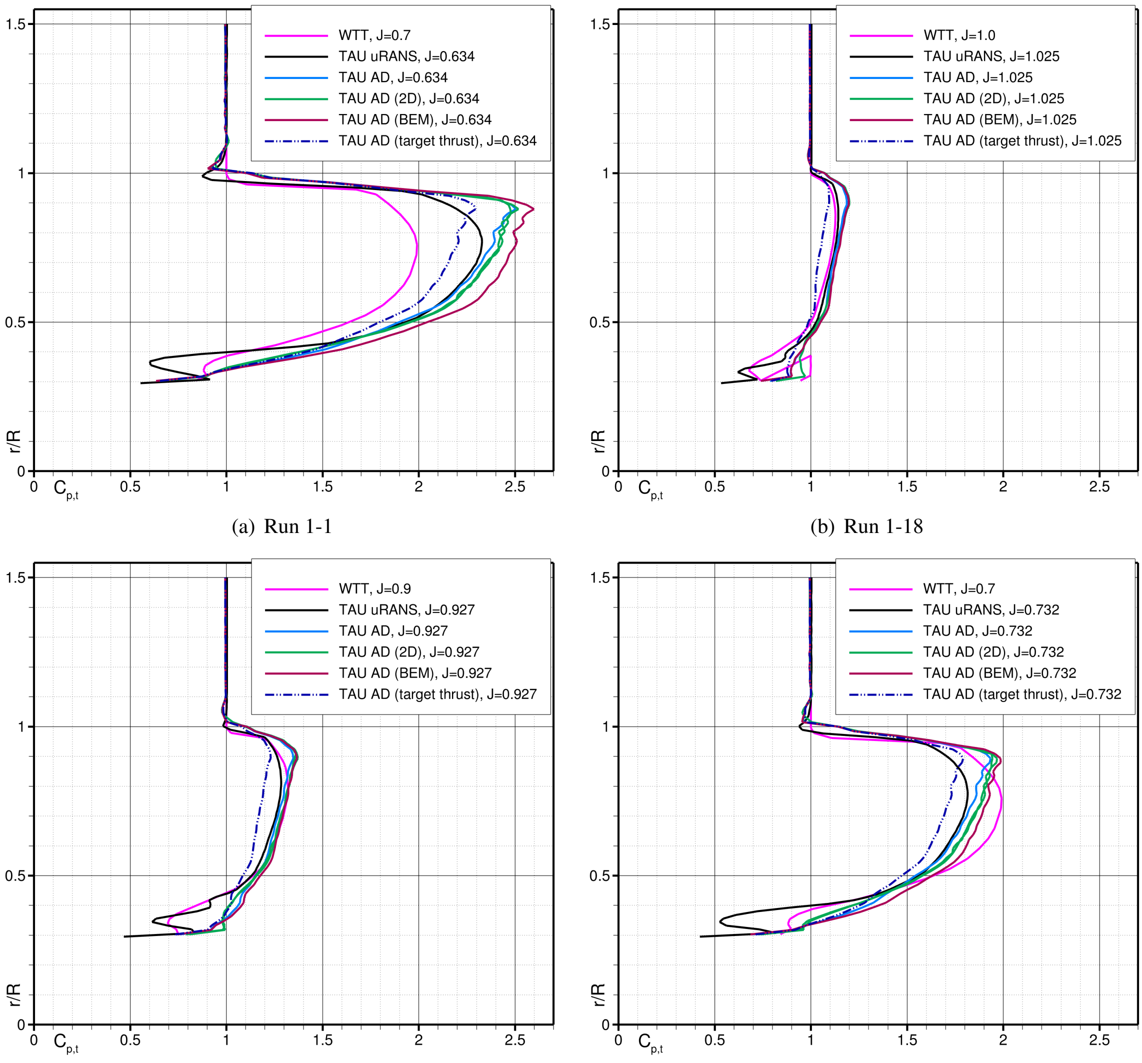

(a) Run 1-1

(b) Run 1-18

(c) Run 1-23

(d) Run 2-2

Figure 9: Comparison of AD modeling impact on the radial $C_{p,t}$ distribution $0.15R$ downstream of the propeller

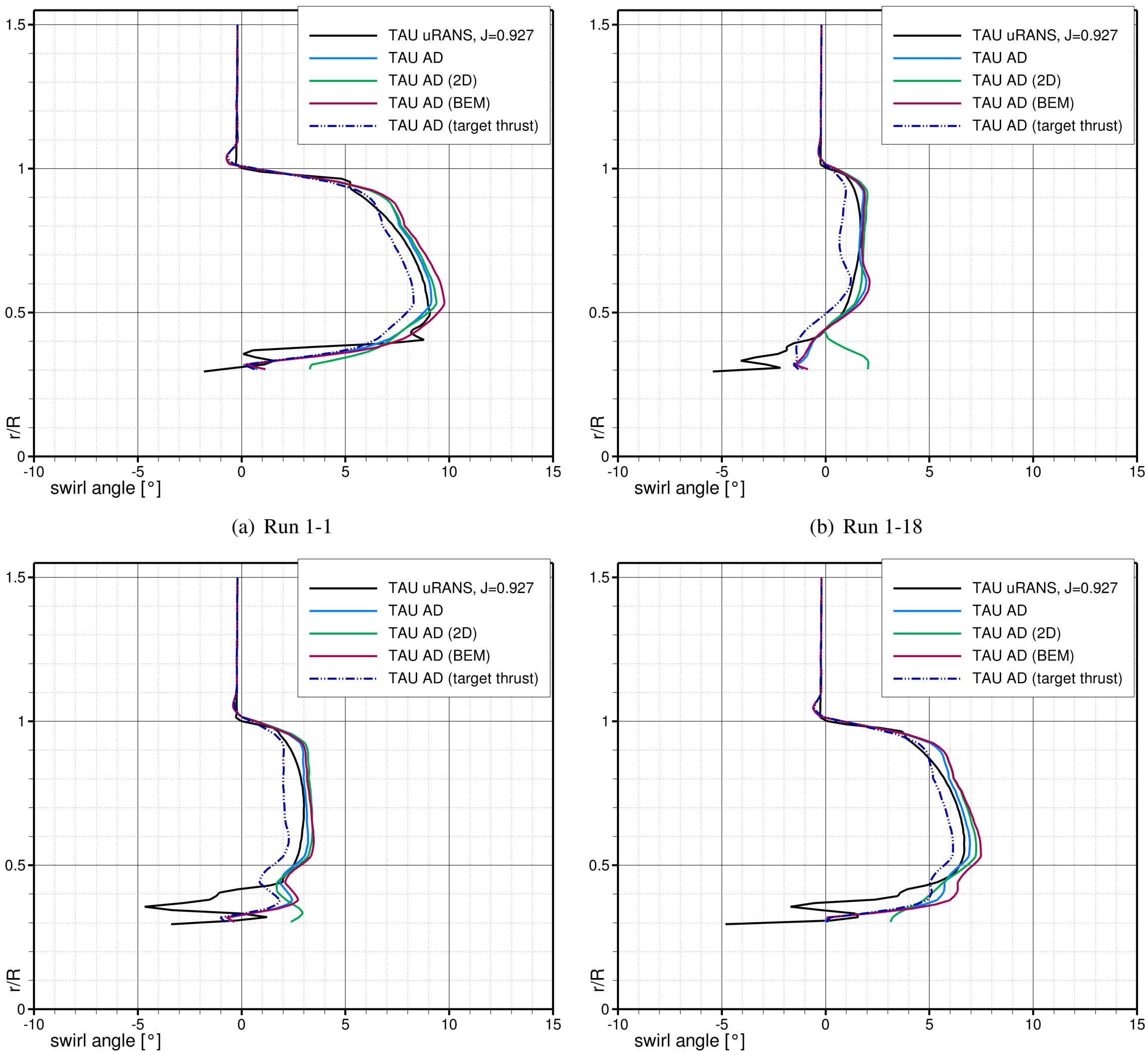

(a) Run 1-1 (b) Run 1-18

(c) Run 1-23 (d) Run 2-2

Figure 10: Comparison of AD modeling impact on the radial swirl distribution at $0.15R$ downstream of the propeller